

Technetium-99m-MIBI and Thallium-201 Scintigraphy of Primary Lung Cancer

Yoshihiro Nishiyama, Yukiko Kawasaki, Yuka Yamamoto, Koutarou Fukunaga, Katashi Satoh, Hitoshi Takashima, Motoomi Ohkawa and Masatada Tanabe

Department of Radiology, Kagawa Medical University, Asada General Hospital, Kagawa, Japan

We evaluated the usefulness of ^{99m}Tc -MIBI scintigraphy in primary lung cancer in comparison with ^{201}Tl -chloride scintigraphy. **Methods:** There were 45 patients with primary lung cancer. All patients underwent dual-isotope imaging with ^{201}Tl -chloride and ^{99m}Tc -MIBI. Regions of interest were placed over the tumors (T) and contralateral normal lung tissue (N) on one coronal view in the SPECT, and T/N ratio and retention index were calculated. **Results:** The positive rate was 98% in both the early and delayed images for ^{201}Tl -chloride and 96% in the early and 89% in the delayed image for ^{99m}Tc -MIBI. Both early and delayed T/N ratios for ^{201}Tl -chloride were higher than those for ^{99m}Tc -MIBI. There was no significant correlation between T/N ratio and histological type of tumor in both images. However, in both images, there was a tendency for the early and delayed ratios to increase as the tumor diameter became larger. The retention index of ^{201}Tl -chloride was higher than that of ^{99m}Tc -MIBI. There were no significant differences in the retention index with respect to the histological type and tumor size. **Conclusion:** The results of this preliminary clinical study suggest that ^{99m}Tl -MIBI can depict primary lung cancer similar to ^{201}Tl -chloride. However, T/N ratio and retention index of ^{99m}Tc -MIBI in the tumor areas are significantly lower compared with those of ^{201}Tl -chloride.

Key Words: technetium-99m-MIBI; thallium-201-chloride; lung cancer; dual-isotope imaging

J Nucl Med 1997; 38:1358-1361

Use of ^{201}Tl -chloride SPECT is now attracting attention for detection of the primary lesions in lung cancer and mediastinal lymph node metastasis (1,2). In recent years, however, several ^{99m}Tc -labeled imaging agents have also been under investigation. Labeling with ^{99m}Tc has several advantages over labeling using ^{201}Tl , namely, ^{99m}Tc is continuously available for use, it permits freedom in patient scheduling and the injected concentration is higher. Noncardiac applications of ^{99m}Tc -MIBI (hexakis 2-methoxy isobutyl isonitrile), such as visualization of benign and malignant lung lesions, have also been investigated. In this study, usefulness of ^{99m}Tc -MIBI for tumor detection in primary lung cancer was evaluated in comparison with ^{201}Tl -chloride.

MATERIALS AND METHODS

Patients

There were 45 patients (37 men and 8 women, age range 39–86 yr) including 18 with squamous cell carcinomas, 13 with adenocarcinomas, 11 with small cell carcinomas, 2 with adenosquamous carcinoma and 1 with large cell carcinoma. Diagnosis was made by cytological or histopathological analysis of sputum, computed tomography (CT) guided needle biopsy or endoscopic samples or lobectomy. All patients underwent simultaneous dual-isotope planar and SPECT of the chest imaging with ^{201}Tl -chloride and

^{99m}Tc -MIBI. None of the patients had received radiotherapy or chemotherapy before imaging.

Simultaneous Dual-Isotope Imaging

All patients underwent simultaneous dual-isotope imaging with a large field-of-view gamma camera, with high resolution and parallel hole collimator. This camera was interfaced to a dedicated computer (Odyssey). A dose of 111 MBq of ^{201}Tl -chloride and 600 MBq of ^{99m}Tc -MIBI was injected intravenously. Early SPECT acquisition was performed 15 min after the injection of each radioisotope and planar images for the whole body and the chest were taken. Delayed SPECT images were acquired 2 hr after injection. Planar images for the chest (512×512 matrix) were acquired for 4 min. For SPECT images, 72 projections were obtained using 64×64 matrix for 45 sec per view. Three energy analyzers were used for acquisition, which were set at 71 keV with a 15% window for ^{201}Tl images, 90 keV with a 10% window for scatter images and 140 keV with a 15% window for ^{99m}Tc images. These projection data were processed with a two-dimensional low-pass filter and then corrected for the contamination scatter. Image reconstruction was done using filtered backprojection with a Ramp filter. Transverse, coronal and sagittal sections were reconstructed.

Contamination Scatter Correction for Each Radionuclide

Because this study involved simultaneous dual-isotope imaging, the raw data at the 71 keV window were contaminated by ^{99m}Tc Compton scatter, and the raw data at the 140 keV window included a 167 keV gamma-ray count of ^{201}Tl . Therefore, the raw ^{201}Tl and ^{99m}Tc data were corrected to eliminate such contamination scatter, according to the equations in each pixel. From phantom studies, the scatter correction coefficient, α , was measured to be 1.07, whereas the cross-talk correction coefficient, β , was measured to be 0.14 (3). The corrected counts in the 71 keV window for ^{201}Tl image, a, and in the 140 keV window for ^{99m}Tc image, b, were as follows: $a = A - \alpha C$, $b = B - \beta a$, where A stands for the raw counts in the 71 keV window, B for the raw counts in the 140 keV window and C for the raw counts in the 90 keV window.

Data Analysis

The planar and SPECT images were compared with chest radiographs and CT. Accumulation in lung tumors was evaluated visually by two radiologists. The planar for both anterior and posterior view and SPECT images were classified as positive (uptake above the normal lung tissue) or negative (uptake similar to the surrounding normal lung parenchymal tissue). In the SPECT images, quantitative analysis of the abnormal uptake of the two radiopharmaceuticals was performed by drawing identical regions of interest over the tumor uptake (T) and contralateral lung tissue area (N) on one coronal section, which demonstrated the lesion most clearly was carefully selected of both early and delayed images. The mean regions of interest values (total counts/total pixels) were measured, and the ratios of tumor to contralateral uptake (T/N ratios) were obtained. We called the T/N ratio of early

Received Aug. 16, 1996; revision accepted Jan. 20, 1997.

For correspondence or reprints contact: Yoshihiro Nishiyama, MD, Department of Radiology, Kagawa Medical University, 1750-1 Ikenobe, Mikicho, Kitagun, Kagawa, 761-07 Japan.

TABLE 1
Positive Rates for Thallium-201-Chloride and Technetium-99m-MIBI

Tumor type	²⁰¹ Tl-chloride			^{99m} Tc-MIBI		
	Planar	SPECT		Planar	SPECT	
		Early	Delayed		Early	Delayed
Small	73 (8/11)	100 (11/11)	100 (11/11)	73 (8/11)	100 (11/11)	100 (11/11)
Squamous	67 (12/18)	100 (18/18)	100 (18/18)	67 (12/18)	94 (17/18)	89 (16/18)
Adeno	77 (10/13)	92 (12/13)	92 (12/13)	69 (9/13)	92 (12/13)	85 (11/13)
Adenosquamous	100 (2/2)	100 (2/2)	100 (2/2)	100 (2/2)	100 (2/2)	100 (2/2)
Large	100 (1/1)	100 (1/1)	100 (1/1)	100 (1/1)	100 (1/1)	100 (1/1)
Total	73% (33/45)	98% (44/45)	98% (44/45)	71% (32/45)	96% (43/45)	89% (40/45)

Small = small-cell carcinoma; Squamous = squamous-cell carcinoma; Adeno = adenocarcinoma; Adenosquamous = adenosquamous cell carcinoma; Large = large-cell carcinoma.

image early ratio and the T/N ratio of delayed image delayed ratio. We quantitatively evaluated the degree of retention in the lesion as follows: (delayed ratio-early ratio) × 100/early ratio. Using this formula, the retention index was obtained. These parameters were compared with tumor histology and tumor size. Tumor sizes were obtained either from pathological specimen or CT imaging measurement. The value of T/N ratio and retention index were expressed as mean ± s.d. To test for differences between these parameters, the Student's t-test was used. Results were considered significant when the p value was below 0.05.

RESULTS

In the planar images, the positive rate was 73% (33/45) for ²⁰¹Tl-chloride and 71% (32/45) for ^{99m}Tc-MIBI. In the SPECT images, the positive rate was 98% (44/45) in both the early and delayed images for ²⁰¹Tl-chloride and 96% (43/45) in the early and 89% (40/45) in the delayed images for ^{99m}Tc-MIBI (Table 1). In the coronal SPECT images, there was a significant difference between the early ratios for ²⁰¹Tl-chloride (3.3 ± 1.2) and ^{99m}Tc-MIBI (2.6 ± 1.1) (p < 0.01). The delayed ratio was 3.8 ± 1.7 for ²⁰¹Tl-chloride and 2.4 ± 1.1 for ^{99m}Tc-MIBI, and this difference was also significant (p < 0.0001). There were no significant differences in early and delayed ratios among three different histologies of lung cancer for both ²⁰¹Tl-chloride and ^{99m}Tc-MIBI (Table 2). In comparison with tumor size, there was a tendency for the early and delayed ratios to increase as the tumor diameter became larger for both ²⁰¹Tl-chloride and ^{99m}Tc-MIBI (Table 3). The retention index was 16.7 ± 31.1 for ²⁰¹Tl-chloride and -10.5 ± 17.2 for ^{99m}Tc-MIBI, and this difference was statistically significant (p < 0.0001). There were no significant differences in retention index among three different histologies of lung cancer for both ²⁰¹Tl-chloride and ^{99m}Tc-MIBI (Table 2). There were no significant differences among tumor size with respect to retention index for ²⁰¹Tl-chloride and ^{99m}Tc-MIBI (Table 3).

Case 1

A 70-yr-old man complained of a persistent mild fever. The chest radiograph showed a 1.0 × 1.0 cm abnormal shadow at the upper part of the left lung (Fig. 1A). Both ²⁰¹Tl-chloride and ^{99m}Tc-MIBI SPECT demonstrated abnormal accumulation corresponding to the lesion on both early and delayed images (Fig. 2B). However, the delayed images of both ²⁰¹Tl-chloride and ^{99m}Tc-MIBI showed fading radioactivity of the lesion compared to that of the early images. No abnormal accumulation was noted in the mediastinum. Early ratio, delayed ratio and retention index for ²⁰¹Tl-chloride were 3.5, 3.2 and -8.6, respectively, and 2.0, 1.8 and -10.0, respectively, for ^{99m}Tc-MIBI. Operative findings proved a 1.0 × 1.0 × 1.5 cm squamous cell carcinoma in S³ of the left lung with the pathological stage as T1 N0 M0.

Case 2

A 59-yr-old man complained of a bloody sputum. The chest radiograph showed a large abnormal shadow at the middle part of the right lung (Fig. 2A). Thallium-201-chloride SPECT showed an abnormal accumulation corresponding to the lesion (Fig. 2B). Early ratio, delayed ratio and retention index for ²⁰¹Tl-chloride were 2.3, 2.9 and 26.1, respectively. However, ^{99m}Tc-MIBI SPECT did not show an abnormal accumulation. No abnormal accumulation was noted in the mediastinum on both ²⁰¹Tl-chloride and ^{99m}Tc-MIBI SPECT. Operative findings proved a 5 × 3.5 × 3 cm adenocarcinoma in S³ of the right lung with the pathological stage as T3 N0 M0.

DISCUSSION

There have been many attempts to use nuclear medicine procedures to overcome the limitations of morphological imaging such as CT or magnetic resonance imaging and the invasiveness of thoracoscopy. Although the number of radio-pharmaceuticals proposed for tumor imaging is in the hundreds,

TABLE 2
Early, Delayed Ratios and Retention Index for Thallium-201-Chloride and Technetium-99m-MIBI According to Tumor Histology

Tumor histology	²⁰¹ Tl-chloride			^{99m} Tc-MIBI		
	ER	DR	RI	ER	DR	RI
Small	3.7 ± 1.2	4.0 ± 1.8	11.0 ± 34.7	3.0 ± 1.1	2.9 ± 1.1	-3.1 ± 22.0
Squamous	3.4 ± 1.1	3.8 ± 1.6	11.3 ± 24.6	2.5 ± 0.9	2.2 ± 0.9	-10.2 ± 15.6
Adeno	3.0 ± 1.3	3.8 ± 2.0	24.0 ± 37.8	2.7 ± 1.4	2.2 ± 1.4	-16.7 ± 15.2

Small = small-cell carcinoma; Squamous = squamous-cell carcinoma; Adeno = adenocarcinoma; ER = early ratio; DR = delayed ratio; RI = retention index.

TABLE 3

Early, Delayed Ratios and Retention Index for Thallium-201-Chloride and Technetium-99m-MIBI According to Tumor Size

Tumor size	²⁰¹ Tl-chloride			^{99m} Tc-MIBI		
	ER	DR	RI	ER	DR	RI
3 cm ≥	2.6 ± 1.0*	3.1 ± 1.8	16.2 ± 36.4	2.1 ± 1.3 [†]	1.9 ± 1.4 [‡]	-13.2 ± 15.6
6 cm >	3.1 ± 0.9 [†]	3.5 ± 1.3	17.2 ± 27.6	2.4 ± 0.8 [§]	2.1 ± 0.8	-12.0 ± 17.8
6 cm ≤	4.0 ± 1.2* [†]	4.6 ± 1.8	16.5 ± 33.0	3.3 ± 1.0 ^{§§}	3.0 ± 0.9 ^{**}	-7.0 ± 18.0

*p < 0.01.

†p < 0.05.

‡p < 0.05.

§p < 0.01.

||p < 0.05.

**p < 0.01.

ER = early ratio; DR = delayed ratio; RI = retention index.

only two simple cations, ⁶⁷Ga and ²⁰¹Tl, have achieved widespread acceptance in clinical imaging (1). Recently, ^{99m}Tc-MIBI has also been reported to be localized in several tumors including lung tumors (4-10). In the study by Hassan et al., the uptake of ^{99m}Tc-MIBI was evaluated in 13 patients with malignant lesions of lung and mediastinum in the planar image (4). However, use of dual-isotope SPECT imaging in primary lung cancers has not been reported. We assessed the clinical utility of ^{99m}Tc-MIBI in patients with primary lung cancer. The results demonstrate that the positive rate was 98% in both the early and delayed SPECT images for ²⁰¹Tl-chloride and 96% in the early and 89% in the delayed SPECT images for ^{99m}Tc-MIBI. Aktolun et al. reported that in malignant tumors the sensitivity of ^{99m}Tc-MIBI was 82.3% and for ²⁰¹Tl-chloride 76.4% (5). In that study, no focal accumulation of ²⁰¹Tl-chloride was detected, whereas ^{99m}Tc-MIBI was detected in the patient with breast cancer. Furthermore, the sensitivity of ^{99m}Tc-MIBI was slightly higher than that of ²⁰¹Tl-chloride (5). This is in contrast with our results. One of the reasons is thought to be the difference in the type of cancer between the two studies.

Shirakawa et al. reported that the T/N ratio of ^{99m}Tc-MIBI in primary lung cancer was 1.94 (6). In this study, we compared both early and delayed SPECT images of ^{99m}Tc-MIBI and ²⁰¹Tl-chloride. The early ratio for ²⁰¹Tl-chloride was significantly higher than that for ^{99m}Tc-MIBI (p < 0.01). The delayed ratio for ²⁰¹Tl-chloride was also significantly higher than that for ^{99m}Tc-MIBI (p < 0.0001).

With respect to the histological type of lung cancer, Togawa et al. reported that adenocarcinoma showed a higher accumulation than squamous cell carcinoma and small cell carcinoma

on the planar images 30 min after intravenous injection of ²⁰¹Tl-chloride (11). Tonami et al. reported that ²⁰¹Tl-chloride clearance in squamous cell carcinoma was faster than that in adenocarcinoma and small cell carcinoma on both early (15 min) and delayed (3 hr) SPECT images after intravenous injection of ²⁰¹Tl-chloride (2). It is interesting that there seems to be a difference in ²⁰¹Tl-chloride accumulation among histological tumor types. When ²⁰¹Tl-chloride was used before biopsy, fewer invasive procedures were performed. However, in our study, there was no significant correlation between T/N ratio and histological type of tumor in both ²⁰¹Tl-chloride and ^{99m}Tc-MIBI images.

Namba et al. reported that there was a tendency for the retention index to increase as the tumor diameter became larger, and the early and delayed ratios also showed a similar trend to the retention index (12). In this study, the early and delayed ratios for both ²⁰¹Tl-chloride and ^{99m}Tc-MIBI showed a tendency to increase with an increase in tumor diameter, but the retention index was not correlated with tumor size. Detectability of a tumor is dependent on the tumor size. The smallest lung cancer in this study, a 1.0 × 1.0 × 1.5 cm squamous cell carcinoma on both dual SPECT, was clearly demonstrated. It is difficult to visualize smaller lesions of lung cancer, and it should therefore not be used as a screening method.

The mechanism of ²⁰¹Tl-chloride uptake in the cell has been reported to be related to the sodium-potassium adenosine triphosphatase (ATPase) pump system (13,14). Thallium-201-chloride behaves like potassium in the metabolic cycle for the release of energy, and its uptake is blocked by ouabain (15). The mechanism of ^{99m}Tc-MIBI uptake is different from that of ²⁰¹Tl-chloride. The uptake of ^{99m}Tc-MIBI is not blocked by

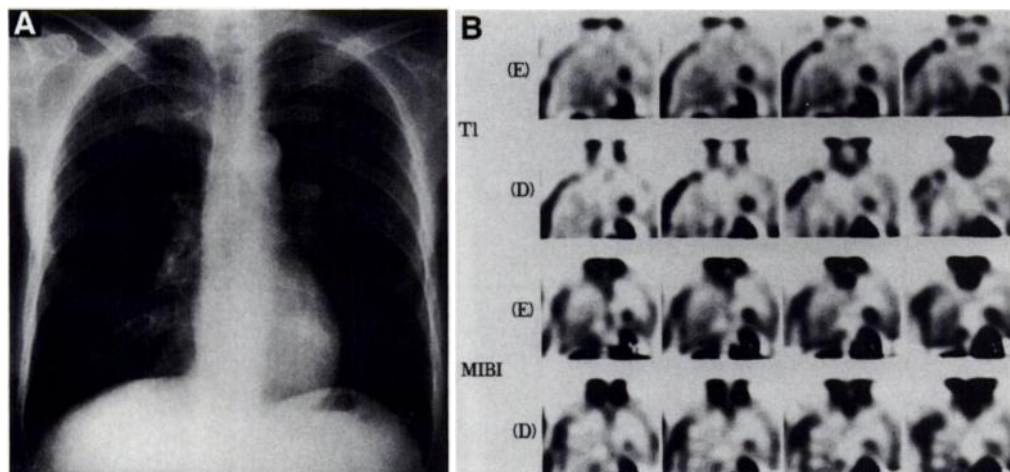


FIGURE 1. Case 1. (A) Chest radiograph showing an abnormal shadow at the upper part of the left lung. (B) Coronal SPECT images of both ²⁰¹Tl-chloride and ^{99m}Tc-MIBI SPECT show an abnormal accumulation corresponding to the lesion. Abnormal accumulation of the lesion is more prominent on early images of both ²⁰¹Tl-chloride and ^{99m}Tc-MIBI than on delayed images. E = early image; D = delayed image.

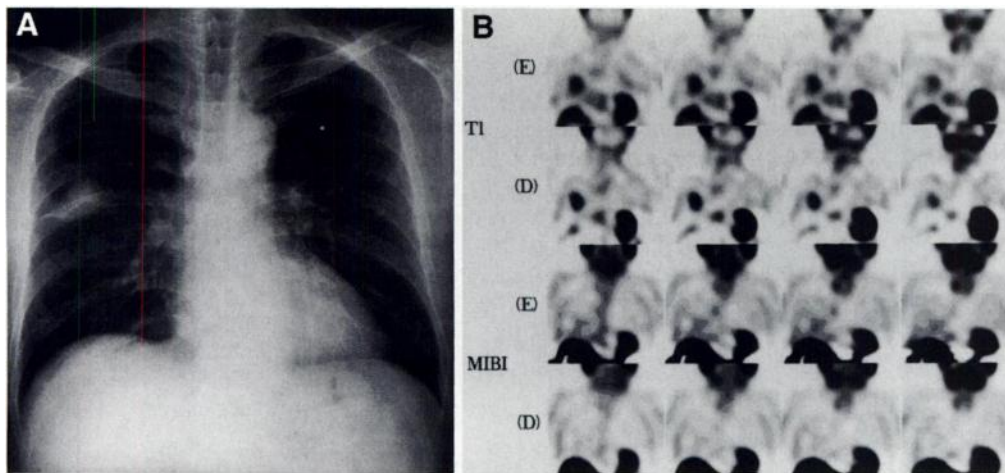


FIGURE 2. Case 2. (A) Chest radiograph showing a large mass shadow at the middle part of the right lung. (B) Early images of ^{201}Tl -chloride SPECT show an abnormal accumulation corresponding to the lesion. Delayed images of ^{201}Tl -chloride SPECT more clearly show the lesion. Technetium-99m-MIBI SPECT did not show an abnormal accumulation corresponding to the lesion in both early and delayed images. E = early image; D = delayed image.

ouabain and is not related to the ATPase system. It has been shown that $^{99\text{m}}\text{Tc}$ -MIBI is attached to a low molecular weight protein in the lysosomes. The cationic charge and lipophilicity of $^{99\text{m}}\text{Tc}$ -MIBI, the mitochondrial and plasma membrane potentials of the tumor cell and the cellular mitochondrial content may play a significant role in the tumor uptake of this agent (16). The uptake may be caused by an indirect mechanism such as increased tumor blood flow and capillary permeability.

In our experience, several patients with benign conditions had a bronchoscopy with biopsy, fine-needle aspiration biopsy and a thoracoscopy because lung cancer could not be ruled out. With reference to the differential diagnosis for pulmonary lesions, the delayed ratio of benign lesions with ^{201}Tl -chloride accumulation was significantly lower than that of lung cancer, and the fading appearance of radioactivity on delayed image was noted in benign lesions (2).

In this study, the T/N ratio of $^{99\text{m}}\text{Tc}$ -MIBI was significantly lower compared with that of ^{201}Tl -chloride on both early and delayed images. The $^{99\text{m}}\text{Tc}$ -MIBI study was not superior to the ^{201}Tl -chloride study for evaluation of the primary lung cancer. However, recent investigations suggest that $^{99\text{m}}\text{Tc}$ -MIBI may interact with P-glycoprotein as a novel organometallic substrate by characterizing the tracer accumulation and inhibition profile in multidrug-resistant cell lines (17–20). The use of $^{99\text{m}}\text{Tc}$ -MIBI is possibly applicable to the prediction of chemotherapeutic efficacy, which is difficult by morphological imaging techniques such as CT and magnetic resonance imaging. Further work in this area, including a study of the relationship between $^{99\text{m}}\text{Tc}$ -MIBI and multidrug resistance, needs to be done.

Kubota et al. (21) reported that PET studies using L-[methyl- ^{11}C]methionine (MET) or ^{18}F -fluorodeoxyglucose (FDG) may be very useful for the differential diagnosis of lung cancer. The L-[methyl- ^{11}C]methionine study showed a sensitivity of 93%, a specificity of 60% and an accuracy of 79%. The ^{18}F -fluorodeoxyglucose study showed 83%, 90% and 86%, respectively. However, to date, there is little information about the comparison of ^{201}Tl -chloride and PET in lung cancer cases. Because of the success achieved by PET but its limited availability, there has been much interest in using SPECT as an alternative imaging technique. Further well-designed studies are required to determine the appropriate role for these studies in the proper management of patients with lung cancer.

CONCLUSION

We can conclude that the $^{99\text{m}}\text{Tc}$ -MIBI study was not superior to the ^{201}Tl -chloride study for evaluation of primary lung cancer. However, $^{99\text{m}}\text{Tc}$ -MIBI is possibly applicable to the prediction of chemotherapeutic efficacy. Technetium-99m-

MIBI scintigraphy, performed in combination with ^{201}Tl -chloride scintigraphy in selected patients, can safely avoid invasive procedures such as biopsy and thoracoscopy.

REFERENCES

- Matsuno S, Tanabe M, Kawasaki Y, et al. Effectiveness of planar image and single photon emission computed tomography of thallium-201 compared with gallium-67 in patients with primary lung cancer. *Eur J Nucl Med* 1992;19:86–95.
- Tonami N, Shuke N, Yokoyama K, et al. Thallium-201 single-photon emission computed tomography in the evaluation of suspected lung cancer. *J Nucl Med* 1989;30:997–1004.
- Yuka Y, Kusuhara T, Kumazawa Y, et al. The effect of scattering in simultaneous acquisitions of technetium-99m and thallium-201: a fundamental study through phantom experiments. *Radioisotopes* 1996;45:369–374.
- Hassan IM, Sahweil A, Constantinides C, et al. Uptake and kinetics of technetium-99m-hexakis 2-methoxy isobutyl isonitrile in benign and malignant lesions in the lungs. *Clin Nucl Med* 1989;14:333–340.
- Actolun C, Bayhan H, Kir M. Clinical experience with technetium-99m-MIBI imaging in patients with malignant tumors: preliminary results and comparison with thallium-201. *Clin Nucl Med* 1992;17:171–176.
- Shirakawa T, Mori Y, Moriya E, et al. Uptake of technetium-99m-hexakis 2-methoxy isobutyl isonitrile in lung or mediastinal lesions by SPECT. *Nippon Acta Radiol* 1995;55:587–592.
- Kao CH, Wang SJ, Lin WY, Hsu CY, Liao SQ, Yeh SH. Differentiation of single solid lesions in the lungs by means of single photon emission tomography with technetium-99m-methoxyisobutylisonitrile. *Eur J Nucl Med* 1993;20:249–254.
- Desai SP, Yuille DL. Visualization of a recurrent carcinoid tumor and an occult distant metastasis by technetium-99m-sestamibi. *J Nucl Med* 1993;34:1748–1751.
- Strouse PJ, Wang DC. Incidental detection of bronchogenic carcinoma during technetium-99m-sestamibi cardiac imaging. *Clin Nucl Med* 1993;18:448–449.
- Cancer B, Kitapci M, Erbenli G, Gogus T, Bekdik C. Increased accumulation of technetium-99m-MIBI in undifferentiated mesenchymal tumor and its metastatic lung lesions. *Clin Nucl Med* 1992;17:144–145.
- Togawa T, Suzuki A, Kato K, et al. Relation between thallium-201 to gallium-67 uptake ratio and histological type in primary lung cancer. *Eur J Cancer Clin Oncol* 1985;21:925–930.
- Namba P, Narabayashi I, Matsui R, et al. Evaluation of thallium-201 SPECT for monitoring the treatment of pulmonary and mediastinal tumors. *Ann Nucl Med* 1995;9:65–74.
- Kishida T. Mechanism of thallium-201 accumulation to thyroid gland: clinical usefulness of dynamic study in thallium-201 chloride scintigraphy for differential diagnosis of thyroid nodules. *Kagu Igaku* 1987;24:991–1004.
- Ito Y, Muranaka A, Harada T, Matsudo A, Yokobayashi T, Terashima H. Experimental study on tumor affinity of thallium-201-chloride. *Eur J Nucl Med* 1978;3:81–86.
- Sehweil AM, McKillop JH, Milroy R, Wilson R, Abdel-Dayem HM, Omar YT. Mechanism of thallium-201 uptake in tumors. *Eur J Nucl Med* 1989;15:376–379.
- Chiu ML, Kronauge JF, Piwnica-Worms D. Effect of mitochondrial and plasma membrane potentials on accumulation of hexakis (2-methoxyisobutylisonitrile) technetium (I) in cultured mouse fibroblasts. *J Nucl Med* 1990;31:1646–1653.
- Ballinger JR, Hua HA, Berry BW, Firby P, Boxen I. Technetium-99m-sestamibi as an agent for imaging P-glycoprotein-mediated multidrug resistance: in vitro and in vivo studies in a rat breast tumor cell line and its doxorubicin-resistant variant. *Nucl Med Commun* 1995;16:253–257.
- Dimitrakopoulou-Strauss A, Strauss LG, Goldschmidt H, Lorenz WJ, Maier-Borst W, Van Kaick G. Evaluation of tumor metabolism and multidrug resistance in patients with treated malignant lymphomas. *Eur J Nucl Med* 1995;22:434–442.
- Rao VV, Chiu ML, Kronauge JF, Piwnica-Worms D. Expression of recombinant human multidrug resistance P-glycoprotein in insect cells confers decreased accumulation of technetium-99m-sestamibi. *J Nucl Med* 1994;35:510–515.
- Komori T, Matsui R, Adachi I, Shimizu T, Sueyoshi K, Narabayashi I. In vitro uptake and release of thallium-201 and technetium-99m-MIBI in HeLa cell. *Kaku Igaku* 1995;32:651–658.
- Kubota K, Matsuzawa T, Fujiwara T, et al. Differential diagnosis of lung tumor with PET: a prospective study. *J Nucl Med* 1990;31:1927–1933.